Progress of Theoretical Physics, Vol. 124, No. 4, October 2010

Baryon-Baryon Interactions in the Flavor $SU(3)$ Limit from Full QCD Simulations on the Lattice

Takashi Inoue,[1,*)] Noriyoshi Ishii,[2] Sinya Aoki,[3,4] Takumi Doi,[3] Tetsuo Hatsuda,[2] Yoichi Ikeda,[5] Keiko Murano,[6] Hidekatsu Nemura[7] and Kenji Sasaki[3]
(HAL QCD Collaboration)

[1]*Nihon University, College of Bioresource Sciences, Fujisawa 252-0880, Japan*
[2]*Department of Physics, University of Tokyo, Tokyo 113-0033, Japan*
[3]*Graduate School of Pure and Applied Sciences, University of Tsukuba, Tsukuba 305-8577, Japan*
[4]*Center for Computational Sciences, University of Tsukuba, Tsukuba 305-8577, Japan*
[5]*Nishina Center for Accelerator-Based Science, Institute for Physical and Chemical Research (RIKEN), Wako 351-0198, Japan*
[6]*High Energy Accelerator Research Organization (KEK), Tsukuba 305-0801, Japan*
[7]*Department of Physics, Tohoku University, Sendai 980-8578, Japan*

(Received July 22, 2010)

We investigate baryon-baryon (BB) interactions in the 3-flavor full QCD simulations with degenerate quark masses for all flavors. The BB potentials in the orbital S-wave are extracted from the Nambu-Bethe-Salpeter wave functions measured on the lattice. We observe strong flavor-spin dependences of the BB potentials at short distances. In particular, a strong repulsive core exists in the flavor-octet and spin-singlet channel (the $\mathbf{8}_s$ representation), while an attractive core appears in the flavor singlet channel (the $\mathbf{1}$ representation). We discuss the relation of such flavor-spin dependence with the Pauli exclusion principle at the quark level. The possible existence of an H-dibaryon resonance above the $\Lambda\Lambda$ threshold is also discussed.

Subject Index: 164, 234

§1. Introduction

The generalized nuclear force, which includes not only the nucleon-nucleon (NN) interaction but also hyperon-nucleon (YN) and hyperon-hyperon (YY) interactions, has been one of the central topics in hadron and nuclear physics. Experimental studies on the ordinary and hyper nuclei[1)] as well as the observational studies of the neutron stars and supernova explosions[2)] are intimately related to the physics of the generalized nuclear force.

As far as the NN interaction is concerned, a significant number of scattering data have been accumulated. Furthermore, the phenomenological NN potential is one of the useful means to parametrize the phase shift data below the meson production threshold: Indeed, the S-wave NN phase shift can be described well by a potential

*) E-mail: inoue.takashi@nihon-u.ac.jp

in the coordinate space with a repulsive core at a short distance and an attractive well at intermediate and long distances.[3)–5)]

In contrast to the NN interaction, properties of the YN and YY interactions are poorly known even today due to the lack of high-precision scattering data for hyperons. The approximate flavor $SU(3)$ symmetry in the hadronic level does not fully constrain the hyperon interactions since there exists six independent flavor channels for the scattering of octet baryons. Theoretical attempts to extract the YN and YY interactions have been made on the basis of the constituent quark models[6)] or the one-boson-exchange models,[7)] but there still exists a large uncertainty in the determination of the generalized nuclear force. To improve this situation, a model independent investigation based on QCD is called for.[8)]

Recently, a new method to extract the baryon-baryon potentials in the coordinate space from lattice QCD simulations has been proposed and applied to the NN system,[9),10)] and ΞN and ΛN systems.[11),12)] In this method, energy-independent nonlocal potentials are defined from the Nambu-Bethe-Salpeter (NBS) amplitude through the Schrödinger equation. In the above studies, it has been shown that the repulsive core at a short distance appears in all NN, ΞN and ΛN systems, while the height and range of the repulsion depend on flavor and spin combinations of two baryons.

The purpose of this paper is to make a systematic study on the short-range baryon-baryon (BB) interactions with full QCD simulations on the lattice. (A preliminary account is given in Ref. 13).) This problem is also closely related to possible dibaryon states such as the flavor-singlet six-quark system H in phenomenological quark models.[14),15)] To capture the essential features of the short range force without contamination from the quark mass difference, we consider the flavor $SU(3)$ limit where all u, d, and s quarks have a common finite mass. This allows us to extract BB potentials for irreducible flavor multiplets, from recombinations of which the potentials between asymptotic baryon states are obtained with suitable Clebsch-Gordan (CG) coefficients.

This paper is organized as follows. In §2, we explain a classification of BB states in the flavor $SU(3)$ limit and a method to extract BB potentials in lattice QCD. In §3, we provide a brief summary of our numerical simulations. In §4, we present the resulting BB potentials and discuss their implications. The last section is devoted to summary and outlook.

§2. Baryon-baryon potentials in the flavor $SU(3)$ limit

In the flavor $SU(3)$ limit, the ground-state baryons belong to the flavor-octet with spin 1/2 or the flavor-decuplet with spin 3/2. In this paper, we focus on the octet baryons, for which two-baryon states with a given angular momentum are labeled by the irreducible flavor multiplets as

$$\mathbf{8} \otimes \mathbf{8} = \underbrace{\mathbf{27} \oplus \mathbf{8}_s \oplus \mathbf{1}}_{\text{symmetric}} \ \underbrace{\oplus \mathbf{10}^* \oplus \mathbf{10} \oplus \mathbf{8}_a}_{\text{antisymmetric}} . \tag{1}$$

Here, "symmetric" and "antisymmetric" stand for the symmetry under the flavor exchange of two baryons. For the system in the orbital S-wave, the Pauli principle between two baryons imposes **27**, $\mathbf{8}_s$ and **1** to be spin singlet ($^1S_0$), while $\mathbf{10}^*$, **10** and $\mathbf{8}_a$ to be spin triplet ($^3S_1$). Since there are no mixings among different multiplets in the $SU(3)$ limit, one can define the corresponding potentials as

$$^1S_0 \ : \ V^{(\mathbf{27})}(r),\ V^{(\mathbf{8}_s)}(r),\ V^{(\mathbf{1})}(r), \tag{2}$$

$$^3S_1 \ : \ V^{(\mathbf{10}^*)}(r),\ V^{(\mathbf{10})}(r),\ V^{(\mathbf{8}_a)}(r)\ . \tag{3}$$

Potentials among octet baryons, both the diagonal part ($B_1B_2 \to B_1B_2$) and the off-diagonal part ($B_1B_2 \to B_3B_4$), are obtained by suitable combinations of $V^{(\alpha)}(r)$ with $\alpha = \mathbf{27}, \mathbf{8}_s, \mathbf{1}, \mathbf{10}^*, \mathbf{10}, \mathbf{8}_a$.

According to Refs. 9) and 10), the above potentials can be defined from the NBS wave function $\phi^{(\alpha)}(\vec{r})$ through the Schrödinger equation as

$$\left[\frac{\nabla^2}{2\mu} + E^{(\alpha)}\right] \phi^{(\alpha)}(\vec{r}) = \int d^3\vec{r}\,' \, U^{(\alpha)}(\vec{r}, \vec{r}\,') \, \phi^{(\alpha)}(\vec{r}\,'), \tag{4}$$

with $E^{(\alpha)} = k^2/(2\mu)$ and $k^2 = W^2/4 - M^2/4$. Here, $\mu = m/2$, $M = 2m$ and W are the reduced mass, total mass and the total energy in the center of mass frame of the two-baryon system with m being the octet baryon mass in the $SU(3)$ limit. Note that $U^{(\alpha)}(\vec{r}, \vec{r}\,')$ is nonlocal but energy-independent and may be written as $U^{(\alpha)}(\vec{r}, \vec{r}\,') = V^{(\alpha)}(\vec{r}, \nabla)\delta^3(\vec{r} - \vec{r}\,')$.[10] At the leading order of the derivative expansion of $V^{(\alpha)}(\vec{r}, \nabla)$,[10),16)] we obtain an effective central potential*)

$$V^{(\alpha)}(\vec{r}) = \frac{1}{2\mu}\frac{\nabla^2\phi^{(\alpha)}(\vec{r})}{\phi^{(\alpha)}(\vec{r})} + E^{(\alpha)}\ . \tag{5}$$

The NBS wave function $\phi^{(\alpha)}$ is defined by

$$\phi^{(\alpha)}(\vec{r})e^{-Wt} = \langle 0|(BB)^{(\alpha)}(t, \vec{r})|B = 2, \alpha, W\rangle, \tag{6}$$

where $(BB)^{(\alpha)}(t, \vec{r}) = \sum_{i,j,\vec{x}} C_{ij} B_i(t, \vec{x} + \vec{r}) B_j(t, \vec{x})$ is a two-baryon operator with relative distance $\vec{r}$ in α-plet and $|B = 2, \alpha, W\rangle$ is a QCD eigenstate with the total energy W and the baryon number 2 in the α-representation. Here, B_i is a one-baryon composite field operator in the octet. The relations between two-baryon operators in the flavor basis and baryon basis are given in Appendix A. In the lattice QCD simulations, the above NBS wave function for the smallest W is extracted from the four-point function as

$$G_4^{(\alpha)}(t - t_0, \vec{r}) = \langle 0|\,(BB)^{(\alpha)}(t, \vec{r})\ \overline{(BB)}^{(\alpha)}(t_0)\,|0\rangle \propto \phi^{(\alpha)}(\vec{r})e^{-W(t-t_0)} \tag{7}$$

for $t - t_0 \gg 1$, where $\overline{(BB)}^{(\alpha)}(t_0)$ is a wall source operator at time t_0 to create two-baryon states in α-plet, while $(BB)^{(\alpha)}(t, \vec{r})$ is the sink operator at time t to annihilate two-baryon states.

*) The "effective" central potential is obtained from the NBS wave function without making a decomposition into central and tensor potentials in the leading order of the derivative expansion.[9),10)] In the $^1S_0$ state, the "effective" central potential reduces to the central potential due to the absence of the tensor component.

Table I. Summary of lattice parameters and hadron masses. The value of lattice spacing a is determined from ρ meson mass at the physical light and strange quark masses. Visit the official website of CP-PACS and JLQCD Collaborations.[18]

lattice	β	a [fm]	L [fm]	κ_{uds}	$m_{\rm ps}$ [MeV]	m_B [MeV]	$N_{\rm cfg}$
$16^3 \times 32$	1.83	0.121(2)	1.93(3)	0.13710	1014(1)	2026(3)	700
				0.13760	835(1)	1752(3)	800

§3. Numerical simulations

We employ the gauge configurations generated by CP-PACS and JLQCD Collaborations with the renormalization-group-improved Iwasaki gauge action and the nonperturbatively $O(a)$-improved Wilson quark action.[17] These configurations are provided by the Japan Lattice Data Grid (JLDG) and International Lattice Data Grid (ILDG). Quark propagators are calculated for the spatial wall source at t_0 with the Dirichlet boundary condition in the temporal direction at $t = t_0 \pm 16$ mod 32. In order to enhance the signal, all 32 time slices on each configuration are used as t_0 of the wall source. In addition, we carry out an average over forward and backward propagations in time.

Our lattice parameters are summarized in Table I. The hopping parameters reside around the physical strange quark mass region in 2+1 flavor QCD at the same β.[18] Since the typical range of the BB interactions at this quark mass is about 1 fm or less as shown below, we expect that the small lattice size ($L \simeq 2$ fm) would not affect the short-range part of the BB interactions qualitatively.

In our calculation, the sink operator is projected to the A_1^+ representation of the cubic group, so that the NBS wave function is assumed to be dominated by the S-wave component. We estimate the statistical errors by the jackknife method with a bin size of seven for $\kappa_{uds} = 0.13710$ and eight for $\kappa_{uds} = 0.13760$. All these numerical computations have been carried out at the KEK supercomputer system, Blue Gene/L and SR11000.

§4. Results and their implications

4.1. *BB potentials in flavor basis*

Figure 1 shows the NBS wave functions as a function of the relative distance between two baryons at $m_\pi = 835$ MeV and $t - t_0 = 10$. To draw all data in the same scale, they are normalized to 1/2 for the singlet channel and to 1 for other channels at the maximum distance. Since the effective mass of the four-point function in each channel shows a plateau at $t - t_0 \geq 10$, we use data at $t - t_0 = 10$ exclusively to extract both NBS wave functions and BB potentials throughout this paper. The wave functions in Fig. 1 show characteristic flavor dependence: In particular, a strong suppression at a short distance appears in the $\mathbf{8}_s$ channel, while a strong enhancement appears in the $\mathbf{1}$ channel. Similar results are also obtained for $m_\pi = 1014$ MeV.

Figure 2 shows the resulting six BB potentials in the flavor basis obtained from the NBS wave functions. Red bars (green crosses) correspond to the pion mass of

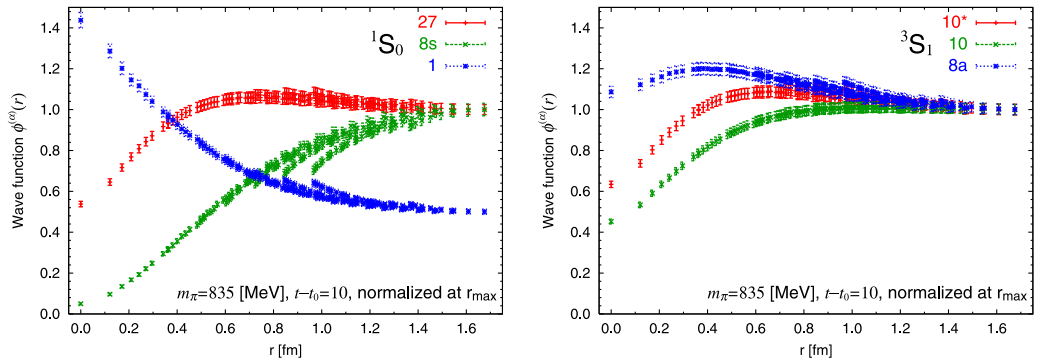

Fig. 1. NBS wave functions at $m_\pi = 835$ MeV and $t - t_0 = 10$, normalized to 1/2 for the singlet channel and to 1 for other channels at the maximum distance.

Table II. Baryon pairs in an irreducible flavor $SU(3)$ representation, where $\{BB'\}$ and $[BB']$ denote $BB' + B'B$ and $BB' - B'B$, respectively.

flavor multiplet	baryon pair (isospin)
27	$\{NN\}(I=1)$, $\{N\Sigma\}(I=3/2)$, $\{\Sigma\Sigma\}(I=2)$, $\{\Sigma\Xi\}(I=3/2)$, $\{\Xi\Xi\}(I=1)$
$\mathbf{8}_s$	none
1	none
$\mathbf{10}^*$	$[NN](I=0)$, $[\Sigma\Xi](I=3/2)$
10	$[N\Sigma](I=3/2)$, $[\Xi\Xi](I=0)$
$\mathbf{8}_a$	$[N\Xi](I=0)$

1014 MeV (835 MeV): Although there is a tendency that the magnitude (range) of the potentials becomes larger at short distances (longer at large distances) for lighter quark mass, the differences are not substantial for the present heavy quark masses.

The three panels on the left show potentials in the $^1S_0$ channel, while those on the right show effective central potentials in the $^3S_1$ channel. We have estimated the energies $E^{(\alpha)}$ under the condition that Eq. (5) approaches zero at large r (the method called "from V" in Ref. 19)). We find $E^{(\mathbf{27})} \simeq -5$ MeV, $E^{(\mathbf{8}_s)} \simeq 25$ MeV, $E^{(\mathbf{1})} \simeq -30$ MeV, $E^{(\mathbf{10}^*)} \simeq -10$ MeV, $E^{(\mathbf{10})} \simeq 0$ MeV and $E^{(\mathbf{8}_a)} \simeq -15$ MeV. Since the constant term (the second term on the right-hand side of Eq. (5)) is small compared to the Laplacian term (the first term on the right-hand side of Eq. (5)) at a short distance, we have not attempted to extract a precise value of $E^{(\alpha)}$ in this study.

Some of the octet-baryon pairs belong exclusively to one irreducible representation, as shown in Table II. For example, a symmetric NN belongs to **27** so that one can regard $V^{(\mathbf{27})}$ as an $SU(3)$ limit of the NN $^1S_0$ potential. Similarly, $V^{(\mathbf{10}^*)}$, $V^{(\mathbf{10})}$ and $V^{(\mathbf{8}_a)}$ can be considered as the $SU(3)$ limits of some potentials in the baryon basis, while $V^{(\mathbf{8}_s)}$ and $V^{(\mathbf{1})}$ are always superpositions of different potentials in the baryon basis.

The top two panels of Fig. 2 show $V^{(\mathbf{27})}$ and $V^{(\mathbf{10}^*)}$, which correspond to NN $^1S_0$ potential and NN $^3S_1$ potential respectively. Both have a repulsive core at a

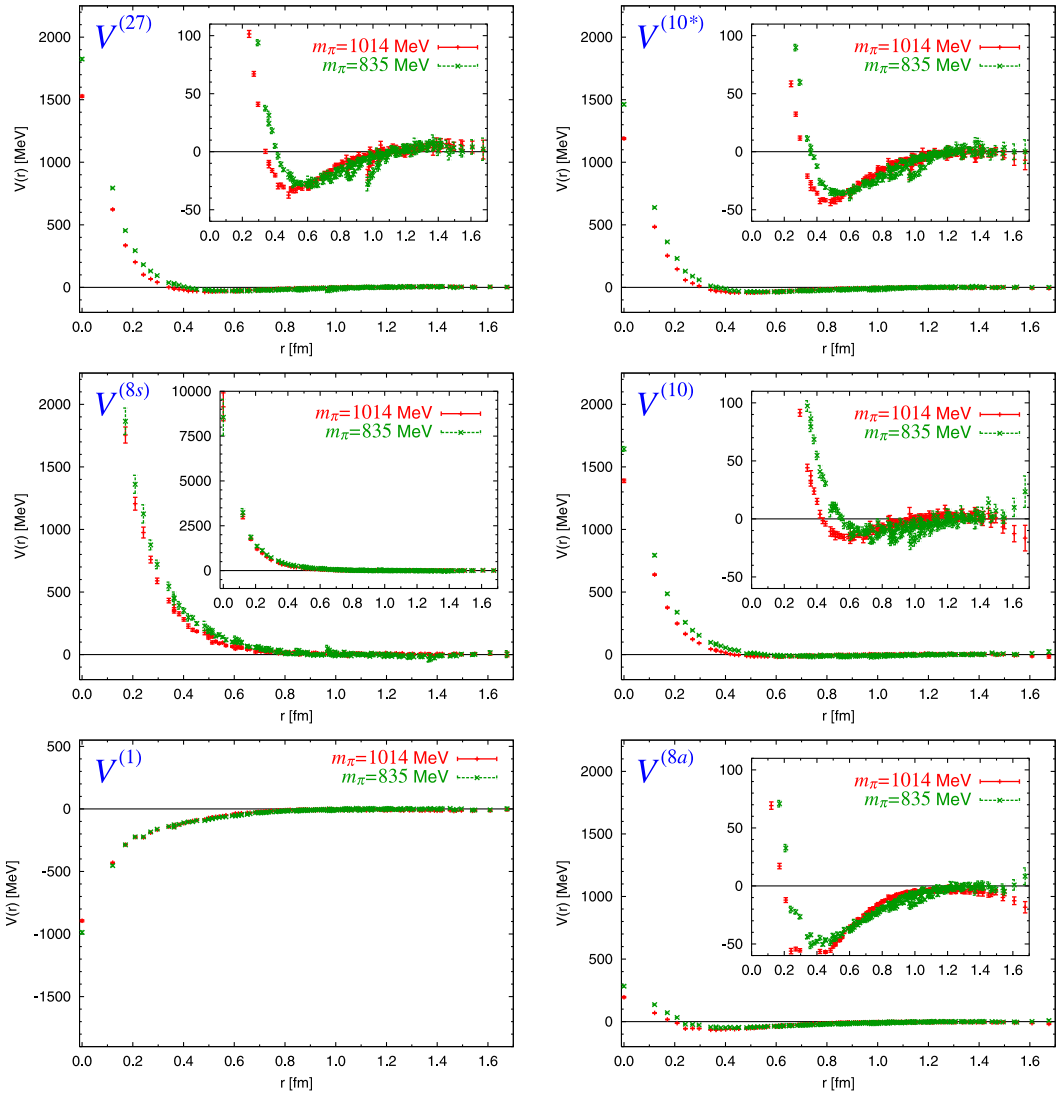

Fig. 2. (color online) Six independent BB potentials for S-wave in the flavor $SU(3)$ limit, extracted from the lattice QCD simulation at $m_\pi = 1014$ MeV (red bars) and $m_\pi = 835$ MeV (green crosses).

short distance and an attractive pocket at around 0.6 fm. These qualitative features are consistent with the previous results found in the NN system in quenched approximation with lighter quark mass.[9] The right middle panel of Fig. 2 shows that $V^{(\mathbf{10})}$ has a stronger repulsive core and a weaker attractive pocket than $V^{(\mathbf{27},\mathbf{10}^*)}$. Furthermore, $V^{(\mathbf{8}_s)}$ in the left middle panel of Fig. 2 has a very strong repulsive core among all the channels, while $V^{(\mathbf{8}_a)}$ in the right bottom panel of Fig. 2 has a very weak repulsive core. In contrast to other cases, $V^{(\mathbf{1})}$ shows attraction for all distances instead of repulsion at a short distance, as shown in the left bottom panel of Fig. 2.

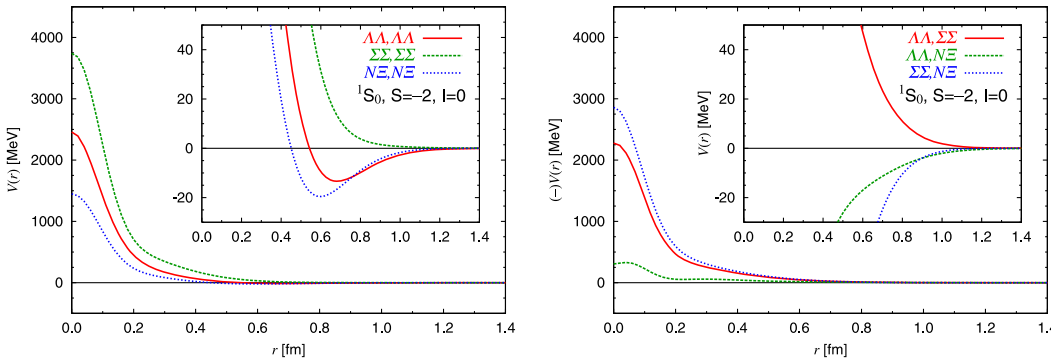

Fig. 3. BB potentials in baryon basis for $S = -2$, $I = 0$, ${}^1S_0$ sector. Three diagonal (off-diagonal) potentials are shown in the left (right) panel. Phases of off-diagonal ones in the right panel are arranged in a zoom-out plot. Their true signs are shown in the insert.

The above features are consistent with what has been observed in phenomenological quark models.[6] In particular, the potential in the $\mathbf{8}_s$ channel in quark models becomes strongly repulsive at a short distance since the six quarks cannot occupy the same orbital state due to quark Pauli blocking. On the other hand, the potential in the $\mathbf{1}$ channel does not suffer from the quark Pauli blocking and can become attractive due to short-range gluon exchange. Such an agreement between the lattice data and the phenomenological models suggests that the quark Pauli blocking plays an essential role in the repulsion in BB system as originally proposed in Ref. 20).

4.2. *BB potentials in baryon basis*

The BB potentials in the baryon basis can be obtained by a unitary rotation of those in the flavor basis. Its explicit form reads,

$$V_{ij}(r) = \sum_{\alpha} U_{i\alpha}\, V^{(\alpha)}(r)\, U^{\dagger}_{\alpha j}, \tag{8}$$

where U is a unitary matrix that rotates the flavor basis $\{\langle\alpha|\}$ to baryon basis $\{\langle i|\}$, i.e., $\langle i| = \sum_\alpha U_{i\alpha}\langle\alpha|$. The explicit forms of the unitary matrix U in terms of the CG coefficients are given in Appendix B.

In Fig. 3, as characteristic examples, we show the potentials for $S = -2$, $I = 0$ sector in the ${}^1S_0$ channel at $m_\pi = 835$ MeV. To obtain $V_{ij}(r)$, we first fit the potentials in the flavor basis by the following form with five parameters $b_1 \sim b_5$,

$$V(r) = b_1 e^{-b_2\, r^2} + b_3(1 - e^{-b_4\, r^2}) \left(\frac{e^{-b_5\, r}}{r}\right)^2. \tag{9}$$

We then use the right-hand side of Eq. (8) to obtain the potentials in the baryon basis. The left panel of Fig. 3 shows the diagonal part of the potentials. The strong repulsion in the $\mathbf{8}_s$ channel is reflected most in the $\Sigma\Sigma(I = 0)$ potential due to its largest CG coefficient among the three channels. The strong attraction in the $\mathbf{1}$ channel is reflected most in the $N\Xi(I = 0)$ potential owing to its largest CG coefficient. Nevertheless, all three diagonal potentials have a repulsive core originating

from the $\mathbf{8}_s$ component. The right panel of Fig. 3 shows the off-diagonal parts of the potential, which are comparable in magnitude to the diagonal ones. Since the off-diagonal parts are not negligible in the baryon basis, full coupled channel analysis is necessary to study the observables. A similar situation holds in 2+1 flavors: The flavor basis with approximately diagonal potentials is useful for obtaining the essential features of the BB interactions, while the baryon basis with a substantial magnitude of the off-diagonal potentials is necessary for practical applications.

Other potentials in baryon basis are given in Fig. 4. Since the $\mathbf{8}_s$ state does not couple to the ${}^3S_1$ channel, the repulsive cores in the ${}^3S_1$ channels (right panels of Fig. 4) are relatively small. The off-diagonal potentials are generally not small: In the right second panel of Fig. 4, for example, the $N\Lambda$-$N\Sigma$ potential in the ${}^3S_1$ channel is comparable in magnitude at short distances to the diagonal $N\Lambda$-$N\Lambda$ and $N\Sigma$-$N\Sigma$ potentials. Although all quark masses of 3 flavors are degenerate and rather heavy in our simulations, these coupled channel potentials in the baryon basis may provide useful hints on the behavior of hyperons (Λ, Σ and Ξ) in hypernuclei and in neutron stars.[1),2)]

§5. Summary and outlook

We have performed 3-flavor full QCD simulations to study the general features of the BB interaction in the flavor $SU(3)$ limit. From the NBS wave function measured on the lattice, we extracted all six independent potentials in the S-wave at the leading order of the derivative expansion: $V^{(\mathbf{27})}$, $V^{(\mathbf{8}_s)}$, $V^{(\mathbf{1})}$, $V^{(\mathbf{10}^*)}$, $V^{(\mathbf{10})}$ and $V^{(\mathbf{8}_a)}$ labeled by flavor irreducible representation. We have found strong flavor dependence of the BB interactions. In particular, $V^{(\mathbf{8}_s)}$ has a very strong repulsive core at a short distance, while $V^{(\mathbf{1})}$ is attractive at all distances. These features are qualitatively consistent with the Pauli blocking effect among quarks previously studied in phenomenological quark models. Recently, the existence (absence) of the repulsive core in the K^+-P potential[21)] (in the $\bar{c}c$-N potential[22)]) has been observed using the same method adopted in this paper. These results further support the relevance of the Pauli blocking effect at the quark level for hadron interactions.

The BB potentials in the baryon basis are reconstructed from those in the flavor basis. We have found that the potentials have a weaker repulsive core in ${}^3S_1$ channels than in ${}^1S_0$ channels, since the $\mathbf{8}_s$ state, which has the strongest repulsive core, does not mix with the former. We note that the off-diagonal potentials are not generally small compared to the diagonal ones. This information together with the future lattice simulations at nondegenerate quark masses in larger volumes will provide useful hints on the structure of hypernuclei and neutron stars.

The flavor singlet channel has attraction for all distances in our simulation. The present data are insufficient to derive a definite conclusion on the H-dibaryon, because of a single small lattice volume and a large degenerate quark mass. Nevertheless, using the potential $V^{(\mathbf{1})}(r)$ and solving the Schrödinger equation Eq. (4) with $E^{(\mathbf{1})} = -30$ MeV, we find a shallow bound state, which suggests a possibility of a bound H-dibaryon with baryon components $\Lambda\Lambda : \Sigma\Sigma : \Xi N = -\sqrt{1} : \sqrt{3} : \sqrt{4}$ in the $SU(3)$ symmetric world at large quark masses. In the real world, the baryon

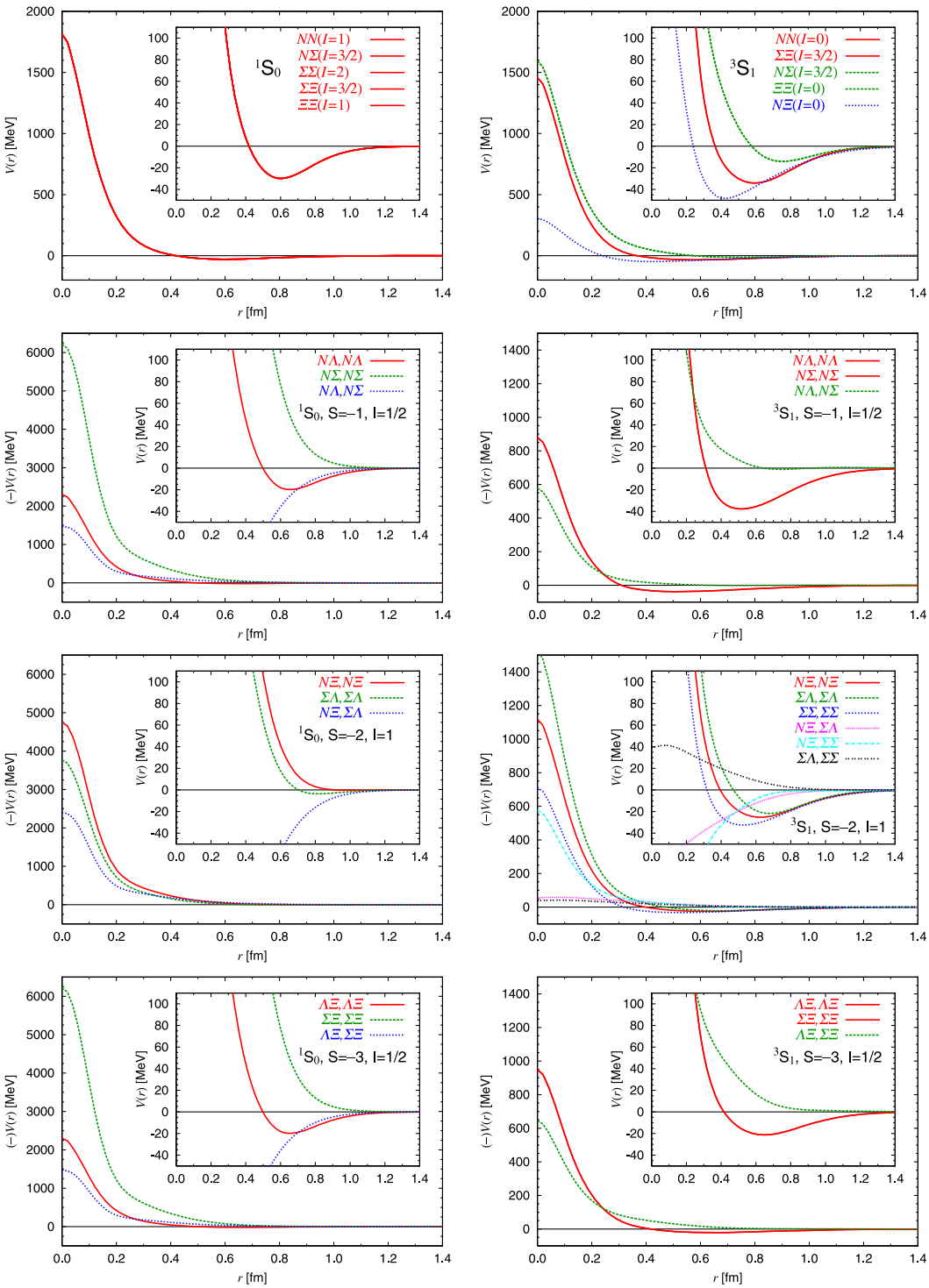

Fig. 4. *BB* potentials in baryon basis other than those shown in Fig. 3. See the caption of Fig. 3.

mass ordering in the $S = -2, I = 0$ sector becomes $\Lambda\Lambda < \Xi N < \Sigma\Sigma$ due to flavor $SU(3)$ breaking. In our trial analysis of solving the Schrödinger equation using the potentials obtained in this paper together with small baryon mass differences from a 2+1 flavor lattice QCD simulation,*) a resonance state is found at an energy between $\Lambda\Lambda$ mass and ΞN mass. If such a resonance exists in nature, it may explain the enhancement just above the $\Lambda\Lambda$ threshold recently reported in the KEK experiment.[23] However, further investigations in both theory and experiment are necessary to drive a definite conclusion.

Acknowledgements

The authors thank the CP-PACS and JLQCD Collaborations for their configurations, the Columbia Physics System[24] for their lattice QCD simulation code, and M. Oka, K. Yazaki, A. Ohnishi, K. Imai, C. Nakamoto, Y. Fujiwara, T. Kawanai and S. Sasaki for helpful discussion and information. This research is supported in part by Grants-in-Aid for Scientific Research on Innovative Areas (Nos. 2004:20105001, 20105003) and the Large Scale Simulation Program No. 09-23 (FY2009) of the High Energy Accelerator Research Organization (KEK). S. A. and T. I. are supported in part by Grant-in-Aid (No. 20340047) of the Ministry of Education, Culture, Sports, Science and Technology. N. I. is supported in part by Grant-in-Aid of MEXT (No. 22540268) and Grant-in-Aid for Specially Promoted Research (13002001). T. D. is supported in part by Grant-in-Aid for JSPS Fellows 21·5985. H. N. is supported in part by MEXT Grant-in-Aid for Scientific Research on Innovative Areas (No. 21105515).

Appendix A
—— *The Irreducible BB Operators* ——

In this Appendix, flavor irreducible BB operators used in this study are given. The composite operators for octet baryons are

$$p_\alpha(x) = +\epsilon_{c_1,c_2,c_3}\,(C\gamma_5)_{\beta_1,\beta_2}\,\delta_{\beta_3,\alpha}\,u(\xi_1)d(\xi_2)u(\xi_3), \tag{A·1}$$

$$n_\alpha(x) = +\epsilon_{c_1,c_2,c_3}\,(C\gamma_5)_{\beta_1,\beta_2}\,\delta_{\beta_3,\alpha}\,u(\xi_1)d(\xi_2)d(\xi_3), \tag{A·2}$$

$$\Sigma^+_\alpha(x) = -\epsilon_{c_1,c_2,c_3}\,(C\gamma_5)_{\beta_1,\beta_2}\,\delta_{\beta_3,\alpha}\,u(\xi_1)s(\xi_2)u(\xi_3), \tag{A·3}$$

$$\Sigma^0_\alpha(x) = -\epsilon_{c_1,c_2,c_3}\,(C\gamma_5)_{\beta_1,\beta_2}\,\delta_{\beta_3,\alpha}\sqrt{\frac{1}{2}}\left[d(\xi_1)s(\xi_2)u(\xi_3) + u(\xi_1)s(\xi_2)d(\xi_3)\right], \tag{A·4}$$

$$\Sigma^-_\alpha(x) = -\epsilon_{c_1,c_2,c_3}\,(C\gamma_5)_{\beta_1,\beta_2}\,\delta_{\beta_3,\alpha}\,d(\xi_1)s(\xi_2)d(\xi_3), \tag{A·5}$$

$$\Xi^0_\alpha(x) = +\epsilon_{c_1,c_2,c_3}\,(C\gamma_5)_{\beta_1,\beta_2}\,\delta_{\beta_3,\alpha}\,s(\xi_1)u(\xi_2)s(\xi_3), \tag{A·6}$$

$$\Xi^-_\alpha(x) = +\epsilon_{c_1,c_2,c_3}\,(C\gamma_5)_{\beta_1,\beta_2}\,\delta_{\beta_3,\alpha}\,s(\xi_1)d(\xi_2)s(\xi_3), \tag{A·7}$$

$$\Lambda_\alpha(x) = -\epsilon_{c_1,c_2,c_3}\,(C\gamma_5)_{\beta_1,\beta_2}\,\delta_{\beta_3,\alpha}$$

*) With hopping parameters $\kappa_{ud} = 0.13760$ and $\kappa_s = 0.13710$ at $\beta = 1.83$, baryon masses are obtained as $M_N = 1797$ MeV, $M_\Lambda = 1827$ MeV, $M_\Sigma = 1833$ MeV, and $M_\Xi = 1860$ MeV.

$$\times\sqrt{\frac{1}{6}}\left[d(\xi_1)s(\xi_2)u(\xi_3)+s(\xi_1)u(\xi_2)d(\xi_3)-2u(\xi_1)d(\xi_2)s(\xi_3)\right] \quad \text{(A·8)}$$

with a notation $\xi_i=\{c_i,\beta_i,x\}$. We follow the phase convention in Ref. 25). In this convention, the two-baryon operator that belongs to the definite flavor representation can be constructed with the Clebsch-Gordan coefficient of $SU(3)$ as

$$BB^{(\mathbf{27})}=+\sqrt{\frac{27}{40}}\Lambda\,\Lambda-\sqrt{\frac{1}{40}}\Sigma\,\Sigma+\sqrt{\frac{12}{40}}N\,\Xi, \quad \text{(A·9)}$$

$$BB^{(\mathbf{8}_s)}=-\sqrt{\frac{1}{5}}\Lambda\,\Lambda-\sqrt{\frac{3}{5}}\Sigma\,\Sigma+\sqrt{\frac{1}{5}}N\,\Xi, \quad \text{(A·10)}$$

$$BB^{(\mathbf{1})}=-\sqrt{\frac{1}{8}}\Lambda\,\Lambda+\sqrt{\frac{3}{8}}\Sigma\,\Sigma+\sqrt{\frac{4}{8}}N\,\Xi, \quad \text{(A·11)}$$

$$BB^{(\mathbf{10}^*)}=+\sqrt{\frac{1}{2}}p\,n-\sqrt{\frac{1}{2}}n\,p, \quad \text{(A·12)}$$

$$BB^{(\mathbf{10})}=+\sqrt{\frac{1}{2}}p\,\Sigma^+-\sqrt{\frac{1}{2}}\Sigma^+\,p, \quad \text{(A·13)}$$

$$BB^{(\mathbf{8}_a)}=+\sqrt{\frac{1}{4}}p\,\Xi^--\sqrt{\frac{1}{4}}\Xi^-\,p-\sqrt{\frac{1}{4}}n\,\Xi^0+\sqrt{\frac{1}{4}}\Xi^0\,n, \quad \text{(A·14)}$$

where $\Sigma\,\Sigma$ and $N\,\Xi$ represent

$$\Sigma\Sigma=+\sqrt{\frac{1}{3}}\Sigma^+\,\Sigma^--\sqrt{\frac{1}{3}}\Sigma^0\,\Sigma^0+\sqrt{\frac{1}{3}}\Sigma^-\,\Sigma^+, \quad \text{(A·15)}$$

$$N\Xi=+\sqrt{\frac{1}{4}}p\,\Xi^-+\sqrt{\frac{1}{4}}\Xi^-\,p-\sqrt{\frac{1}{4}}n\,\Xi^0-\sqrt{\frac{1}{4}}\Xi^0\,n\,. \quad \text{(A·16)}$$

Appendix B

Relation between the Flavor Basis and Baryon Basis

Unitary matrices U that rotates the flavor basis $\{\langle\alpha|\}$ to baryon basis $\{\langle i|\}$ are given as follows.

1. $S=-1$, $I=1/2$, ${}^1S_0$ sector.

$$\begin{pmatrix}\langle N\Lambda|\\ \langle N\Sigma|\end{pmatrix}=\begin{pmatrix}\sqrt{\frac{9}{10}} & -\sqrt{\frac{1}{10}}\\ \sqrt{\frac{1}{10}} & \sqrt{\frac{9}{10}}\end{pmatrix}\begin{pmatrix}\langle\mathbf{27}|\\ \langle\mathbf{8}_s|\end{pmatrix}. \quad \text{(B·1)}$$

2. $S=-1$, $I=1/2$, ${}^3S_1$ sector.

$$\begin{pmatrix}\langle N\Lambda|\\ \langle N\Sigma|\end{pmatrix}=\begin{pmatrix}\sqrt{\frac{1}{2}} & -\sqrt{\frac{1}{2}}\\ \sqrt{\frac{1}{2}} & \sqrt{\frac{1}{2}}\end{pmatrix}\begin{pmatrix}\langle\mathbf{10}^*|\\ \langle\mathbf{8}_a|\end{pmatrix}. \quad \text{(B·2)}$$

3. $S=-2$, $I=0$, ${}^1S_0$ sector.

$$\begin{pmatrix} \langle \Lambda\Lambda| \\ \langle \Sigma\Sigma| \\ \langle N\Xi| \end{pmatrix} = \begin{pmatrix} \sqrt{\frac{27}{40}} & -\sqrt{\frac{8}{40}} & -\sqrt{\frac{5}{40}} \\ -\sqrt{\frac{1}{40}} & -\sqrt{\frac{24}{40}} & \sqrt{\frac{15}{40}} \\ \sqrt{\frac{12}{40}} & \sqrt{\frac{8}{40}} & \sqrt{\frac{20}{40}} \end{pmatrix} \begin{pmatrix} \langle \mathbf{27}| \\ \langle \mathbf{8}_s| \\ \langle \mathbf{1}| \end{pmatrix}. \tag{B·3}$$

4. $S=-2$, $I=1$, ${}^1S_0$ sector.

$$\begin{pmatrix} \langle N\Xi| \\ \langle \Sigma\Lambda| \end{pmatrix} = \begin{pmatrix} \sqrt{\frac{2}{5}} & -\sqrt{\frac{3}{5}} \\ \sqrt{\frac{3}{5}} & \sqrt{\frac{2}{5}} \end{pmatrix} \begin{pmatrix} \langle \mathbf{27}| \\ \langle \mathbf{8}_s| \end{pmatrix}. \tag{B·4}$$

5. $S=-2$, $I=1$, ${}^3S_1$ sector.

$$\begin{pmatrix} \langle N\Xi| \\ \langle \Sigma\Lambda| \\ \langle \Sigma\Sigma| \end{pmatrix} = \begin{pmatrix} -\sqrt{\frac{1}{3}} & -\sqrt{\frac{1}{3}} & \sqrt{\frac{1}{3}} \\ -\sqrt{\frac{1}{2}} & \sqrt{\frac{1}{2}} & 0 \\ \sqrt{\frac{1}{6}} & \sqrt{\frac{1}{6}} & \sqrt{\frac{4}{6}} \end{pmatrix} \begin{pmatrix} \langle \mathbf{10}^*| \\ \langle \mathbf{10}| \\ \langle \mathbf{8}_a| \end{pmatrix}. \tag{B·5}$$

6. $S=-3$, $I=1/2$, ${}^1S_0$ sector.

$$\begin{pmatrix} \langle \Lambda\Xi| \\ \langle \Sigma\Xi| \end{pmatrix} = \begin{pmatrix} \sqrt{\frac{9}{10}} & -\sqrt{\frac{1}{10}} \\ \sqrt{\frac{1}{10}} & \sqrt{\frac{9}{10}} \end{pmatrix} \begin{pmatrix} \langle \mathbf{27}| \\ \langle \mathbf{8}_s| \end{pmatrix}. \tag{B·6}$$

7. $S=-3$, $I=1/2$, ${}^3S_1$ sector.

$$\begin{pmatrix} \langle \Lambda\Xi| \\ \langle \Sigma\Xi| \end{pmatrix} = \begin{pmatrix} \sqrt{\frac{1}{2}} & -\sqrt{\frac{1}{2}} \\ \sqrt{\frac{1}{2}} & \sqrt{\frac{1}{2}} \end{pmatrix} \begin{pmatrix} \langle \mathbf{10}| \\ \langle \mathbf{8}_a| \end{pmatrix}. \tag{B·7}$$

References

1) Reviewed in O. Hashimoto and H. Tamura, Prog. Part. Nucl. Phys. **57** (2006), 564.
2) Reviewed in J. Schaffner-Bielich, Nucl. Phys. A **835** (2010), 279, arXiv:1002.1658.
3) M. Taketani et al., Prog. Theor. Phys. Suppl. No. 39 (1967), 1.
   N. Hoshizaki et al., Prog. Theor. Phys. Suppl. No. 42 (1968), 1.
4) R. Machleidt and I. Slaus, J. of Phys. G **27** (2001), R69, nucl-th/0101056.
5) E. Epelbaum, H. W. Hammer and U. G. Meissner, Rev. Mod. Phys. **81** (2009), 1773, arXiv:0811.1338.
6) Reviewed in M. Oka, K. Shimizu and K. Yazaki, Prog. Theor. Phys. Suppl. No. 137 (2000), 1.
   Y. Fujiwara, Y. Suzuki and C. Nakamoto, Prog. Part. Nucl. Phys. **58** (2007), 439, nucl-th/0607013.
   Y. Fujiwara and Y. Suzuki, Nucl. Phys. News **18N2** (2008), 17.
7) T. A. Rijken, M. M. Nagels and Y. Yamamoto, Nucl. Phys. A **835** (2010), 160.
8) S. Aoki, Nucl. Phys. B (Proc. Suppl.) **195** (2009), 281, arXiv:0910.3801.
   T. Hatsuda, PoS(CD09)068, arXiv:0909.5637.
9) N. Ishii, S. Aoki and T. Hatsuda, Phys. Rev. Lett. **99** (2007), 022001, nucl-th/0611096.
10) S. Aoki, T. Hatsuda and N. Ishii, Prog. Theor. Phys. **123** (2010), 89, arXiv:0909.5585.

11) H. Nemura, N. Ishii, S. Aoki and T. Hatsuda, Phys. Lett. B **673** (2009), 136, arXiv:0806.1094.
12) H. Nemura (HAL QCD and PACS-CS Collaborations), PoS(LAT2009)152.
13) T. Inoue (HAL QCD Collaboration), PoS(LAT2009)133, arXiv:0911.2305.
14) R. L. Jaffe, Phys. Rev. Lett. **38** (1977), 195 [Errata; **38** (1977), 617].
15) Reviewed in T. Sakai, K. Shimizu and K. Yazaki, Prog. Theor. Phys. Suppl. No. 137 (2000), 121, nucl-th/9912063.
16) K. Murano, N. Ishii, S. Aoki and T. Hatsuda, PoS(LAT2009)126, arXiv:1003.0530.
17) T. Ishikawa et al. (JLQCD Collaboration), Phys. Rev. D **78** (2008), 011502, arXiv:0704.1937.
18) CP-PACS and JLQCD Collaboration, `http://www.jldg.org/ildg-data/CPPACS+JLQCDconfig.html`
19) S. Aoki et al. (CP-PACS Collaboration), Phys. Rev. D **71** (2005), 094504, hep-lat/0503025.
20) S. Otsuki, M. Yasuno and R. Tamagaki, Prog. Theor. Phys. Suppl. Extra Number (1965), 578.
S. Machida and M. Namiki, Prog. Theor. Phys. **33** (1965), 125.
V. G. Neudachin, Yu. F. Smirnov and R. Tamagaki, Prog. Theor. Phys. **58** (1977), 1072.
21) Y. Ikeda et al. (HAL QCD Collaboration), arXiv:1002.2309.
22) T. Kawanai and S. Sasaki, arXiv:1007.1515.
23) C. J. Yoon et al. (KEK-PS E522 Collaboration), Phys. Rev. C **75** (2007), 022201.
24) Columbia Physics System (CPS), `http://qcdoc.phys.columbia.edu/cps.html`
25) J. J. de Swart, Rev. Mod. Phys. **35** (1963), 916 [Errata; **37** (1965), 326].